Letter

Quantum-enhanced metrology in cavity magnonics

Qing-Kun Wan,[1,2] Hai-Long Shi,[3,4,*] and Xi-Wen Guan[1,4,5,6,†]

[1]*Innovation Academy for Precision Measurement Science and Technology, Chinese Academy of Sciences, Wuhan 430071, China*
[2]*University of Chinese Academy of Sciences, Beijing 100049, China*
[3]*QSTAR and INO-CNR, Largo Enrico Fermi 2, 50125 Firenze, Italy*
[4]*Hefei National Laboratory, Hefei 230088 China*
[5]*NSFC-SPTP Peng Huanwu Center for Fundamental Theory, Xi'an 710127, China*
[6]*Department of Fundamental and Theoretical Physics, Research School of Physics, Australian National University, Canberra, Australian Capital Territory 0200, Australia*

(Received 20 January 2023; revised 9 December 2023; accepted 21 December 2023; published 16 January 2024)

Magnons, as fundamental quasiparticles that emerge in elementary spin excitations, hold a big promise for innovating quantum technologies in information coding and processing. By establishing the exact relation between Fisher information and entanglement in partially accessible metrological schemes, we rigorously prove that bipartite entanglement plays a crucial role during the dynamical encoding process. However, the presence of an entanglement during the measurement process unavoidably reduces the ultimate measurement precision. These findings are verified in an experimentally feasible cavity magnonic system engineered for detecting a weak magnetic field by performing precision measurements through the cavity field. Moreover, we further demonstrate that, within a weak-coupling region, measurement precision can reach the Heisenberg limit. Additionally, quantum criticality also enables us to enhance measurement precision in a strong-coupling region.

DOI: 10.1103/PhysRevB.109.L041301

Introduction. In contrast to classical estimation theory, quantum metrology seeks a higher-precision estimation of some fundamental physical quantities by using various quantum resources, such as squeezed light [1,2], entanglement [3–9], steering [10–12], nonlocality [13], discord [14–16], etc. In this scenario, quantum information science combined with condensed-matter physics strikingly deepens our understanding of quantum features of quasiparticles and opens a new avenue of implementing quantum-enhanced metrology by virtue of quasiparticles [17–26], for example, quantum metrology at quantum criticality [27–39], and by dynamic structure factor [40,41].

Magnons, as the collective magnetic excitations of the magnetically ordered states in interacting spins, have received increasing attention due to their capability for carrying, transporting, and processing quantum information [42–44]. Appealing features of magnons include their stability at room temperature, high spin density, no ohmic losses, and fine tunability of spin orientations. Promising potential applications have stimulated recent research on cavity magnonics, especially on magnon-photon entanglement and magnon-magnon entanglement [45–59], and the role of entanglement in quantum batteries [60–62]. For quantum metrology, entanglement is known to provide enhanced sensing precision in global parameter estimations requiring also global measurements [4–6]. However, global accessibility is often limited in cavity magnonic systems [63,64]. Natural questions arise: What is the role of bipartite entanglement in partially accessible metrological schemes? Can quantum-enhanced metrology be realized in such cavity magnonic systems?

In this Letter, we address the aforementioned questions by analyzing the influence of bipartite entanglement on the scaling of quantum and classical Fisher information (QFI and CFI), which quantify the measurement precision. We identify two important conditions for enhancing measurement precision: Encoding the estimated parameter within the covariance matrix of the partially accessible quantum state and minimizing thermalization during the final measurement process as well. The former is ensured by the bipartite entanglement generated through quantum dynamics, whereas the latter is to avoid bipartite entanglement in the measurement process. Based on this finding, we verify optimal measurement precisions for different settings in the experimentally feasible cavity magnonic system [65–68]. We show that the Heisenberg limit (HL) can be achieved in the weak-coupling case with an initial squeezed magnon, whereas criticality-enhanced metrology can be realized in the strong-coupling case without a need for quantum squeezing.

Role of entanglement in partially accessible metrological schemes. Partially accessible metrological schemes aim to estimate a parameter B from the subsystem $\hat{\rho}_c \equiv \mathrm{Tr}_m(\hat{\rho}_{cm})$ where c and m represent two distinct subsystems, such as cavity and magnon. Focusing on a pure state for the total system $\hat{\rho}_{cm}$ and assuming a Gaussian state for $\hat{\rho}_c$, we express $\hat{\rho}_c$ as $\hat{\rho}_c = \hat{D}(\alpha)\hat{S}(\zeta)\hat{\rho}_{\mathrm{th}}\hat{S}^{\dagger}(\zeta)\hat{D}^{\dagger}(\alpha)$ [69] in terms of the parameters α, r, ϕ, and n_{th} [70]:

$$\alpha = \frac{1}{\sqrt{2}}\left(d_1^c + i d_2^c\right), \quad r = \frac{1}{2}\mathrm{arcosh}\left(\frac{\mathrm{Tr}(\gamma^c)}{2\sqrt{\det(\gamma^c)}}\right),$$
$$n_{\mathrm{th}} = \frac{\sqrt{\det(\gamma^c)} - 1}{2}, \quad \tan\phi = \left(\frac{2\gamma_{12}^c}{\gamma_{11}^c - \gamma_{22}^c}\right), \tag{1}$$

*hailong.shi@ino.cnr.it
†xiwen.guan@anu.edu.au

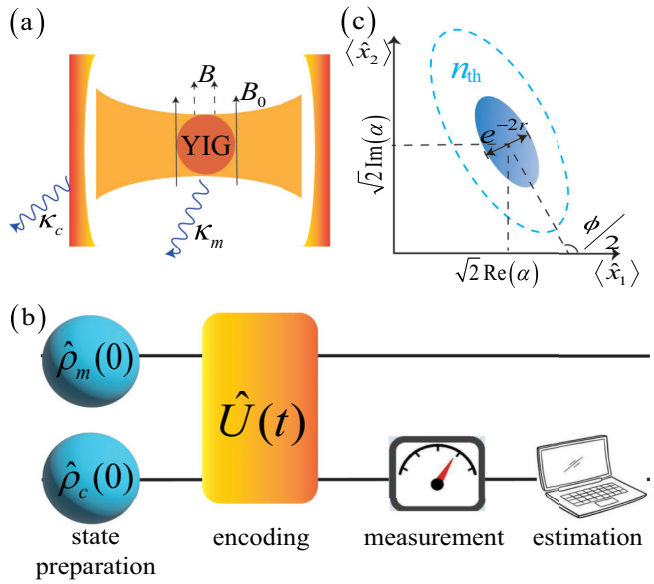

FIG. 1. (a) Schematic illustration of the cavity magnonic system. A YIG sphere is placed in a cavity to sense the weak magnetic field B, with a bias magnetic field B_0 applied for magnon excitation. κ_c and κ_m represent the damping rates of the cavity and the magnon, respectively. (b) Metrological scheme for estimating the parameter B. Quantum dynamics encode the estimated parameter within the covariant matrix, while the measurement is performed on the cavity. (c) Illustration of the Wigner function of a single-mode Gaussian state in terms of displacement, squeezing, phase, and thermalization parameters (α, r, ϕ, $n_{\rm th}$).

where $d_j^c = \langle \hat{x}_j \rangle$ is the displacement vector, $\gamma_{jk}^c = \langle \{\hat{x}_j - \langle \hat{x}_j \rangle, \hat{x}_k - \langle \hat{x}_k \rangle\} \rangle/2$ is the covariance matrix, $\hat{x}_1 = (\hat{c}^\dagger + \hat{c})/\sqrt{2}$, $\hat{x}_2 = i(\hat{c}^\dagger - \hat{c})/\sqrt{2}$, and $\langle \hat{A} \rangle = \mathrm{Tr}(\hat{\rho}_c \hat{A})$. The parameters α, r, ϕ, and $n_{\rm th}$ characterize the displacement, squeezing, phase, and thermalization for subsystem $\hat{\rho}_c$, respectively [see Fig. 1(c)].

The estimation precision provided by $\hat{\rho}_c$ is the Cramér-Rao bound [71–74], i.e., a lower bound $(\delta B)^2 \geqslant 1/F_Q(\hat{\rho}_c)$. In terms of the parameters α, r, ϕ, and $n_{\rm th}$ [75], we analytically derive the QFI (see the Supplemental Material (SM) [76]; see also Refs. [77,78] therein):

$$F_Q(\hat{\rho}_c) = \frac{4}{2n_{\rm th}+1}[\alpha'\bar{\alpha}'\cosh(2r) + \mathrm{Re}(\bar{\alpha}'^2 e^{i\phi})\sinh(2r)] + \frac{n_{\rm th}'^2}{n_{\rm th}(1+n_{\rm th})} + \frac{(1+2n_{\rm th})^2}{2\left(1+2n_{\rm th}+2n_{\rm th}^2\right)} \times [\sinh^2(2r)\phi'^2 + 4r'^2], \tag{2}$$

where $\bar{\alpha}$ is the complex conjugate of α and the prime denotes the derivative with respect to B.

If $\hat{\rho}_c$ does not arise from critical dynamics, it is justifiable to assume finite values for α, r, ϕ, and $n_{\rm th}$ and their respective derivatives. Enhancing measurement precision primarily relies on particle number, i.e., $N_c \equiv |\alpha|^2 + n_{\rm th} + (2n_{\rm th}+1)\sinh^2 r$. We first consider the case where particle number is mainly sourced by the displacement, e.g., a coherent state, $N_c \sim |\alpha|^2$. Then, Eq. (2) implies $F_Q \sim \alpha'\bar{\alpha}'$, leading to the shot noise limit (SNL), i.e., $F_Q \sim N_c$. Here it is reasonable to assume that the parameters and their derivatives are of the same order. In the second case, if the thermalized photons dominate, i.e., $N_c \sim n_{\rm th}$, then QFI (2) does not increase with N_c since $F_Q \sim O(1)$.

Excluding the displacement and thermalized photons as metrological resources, quantum squeezing emerges as a vital resource for surpassing the shot noise limit (also see the study in Refs. [2,79–85]). In the third case, assuming that quantum squeezing is dominant, then $N_c \sim \sinh^2 r \sim e^{2r}$ and $F_Q \sim \sinh^2(2r) \sim e^{4r}$. Explicitly, it achieves the HL, $F_Q \sim N_c^2$. To incorporate the influence of the inevitable thermalization in QFI, we assume the number of thermalized photons scales as $n_{\rm th} \sim e^{\nu r}$ [86]. Equation (2) reveals that the thermalization does not really affect the scaling of QFI if $n_{\rm th}$ dominates. However, $N_c \sim e^{(2+\nu)r}$ can essentially depend on the thermalization. So, QFI exhibits a scaling,

$$F_Q \sim N_c^{4/(2+\nu)}, \tag{3}$$

which can exceed the SNL if $\nu < 2$.

Bipartite entanglement can be quantified by the entanglement entropy $S(t) = -\mathrm{Tr}[\hat{\rho}_c \log_2(\hat{\rho}_c)]$ [87]. For Gaussian states, it reduces to [88]

$$S(t) = \log_2(n_{\rm th}+1) + n_{\rm th}\log_2\left(\frac{n_{\rm th}+1}{n_{\rm th}}\right), \tag{4}$$

showing that entanglement increases with the number of thermalized photons $n_{\rm th}$ grows. Combining Eqs. (3) and (4), we deduce that the existence of bipartite entanglement decreases the final measurement precision. Nevertheless, in order to achieve scaling law (3), the parameters are required to be encoded effectively in the covariance matrix of the subsystem $\hat{\rho}_c$. The emergent entanglement guarantees such an encoding from a product state, thus highlighting the significance of bipartite entanglement in the dynamical encoding process. This finding establishes fundamental laws governing the role of bipartite entanglement in partially accessible Gaussian metrology.

Quantum measurements. Now we discuss how to experimentally realize the measurement precision given by the Cramér-Rao bound. Based on the Gaussian measurements, the CFI is obtained as follows [76] (see also Ref. [89] therein):

$$F_C(\hat{\rho}_c) = \frac{[n_{\rm th}' - (2n_{\rm th}+1)r']^2}{2(n_{\rm th}+1)^2} + \frac{[n_{\rm th}' + (2n_{\rm th}+1)r']^2}{2(n_{\rm th}+1)^2} + \frac{(2n_{\rm th}+1)^2[\phi'\sinh(2r)]^2}{4(n_{\rm th}+1)^2}, \tag{5}$$

where we only considered quantum states with zero displacement. Equation (5) reveals that the scaling of CFI matches that of QFI, demonstrating that Gaussian measurements are optimal. Experimentally, after acquiring probabilities through Gaussian measurements, we can utilize the maximum likelihood estimator to estimate the unknown parameter [90]. Implementing Gaussian measurements involves two steps: Applying a Gaussian unitary operation to the input system, which includes additional ancillary (vacuum) modes, and performing homodyne measurements on all output modes [91–93]. Next, we apply these general results to a cavity magnonic system, exploring distinct roles of entanglement in dynamic encoding and measurement processes.

Model. We consider a system consisting of a yttrium iron garnet (YIG) sphere placed inside a microwave cavity and subjected to a static magnetic field, B_0 [65,66] [see Fig. 1(a)]. The microwave field induces magnon excitations in the ferromagnetic YIG sphere. Additionally, we introduce a weak field B for estimation. Using the Holstein-Primakoff approximation [94], the corresponding Hamiltonian is given by [66,95]

$$\hat{H} = \omega_c \hat{c}^\dagger \hat{c} + \omega_m \hat{b}^\dagger \hat{b} + g(\hat{c} + \hat{c}^\dagger)(\hat{b} + \hat{b}^\dagger), \tag{6}$$

where $\hat{c}^\dagger$ ($\hat{b}^\dagger$) and $\hat{c}$ ($\hat{b}$) are creation and annihilation operators for the cavity photon (magnon) at frequency ω_c [$\omega_m = \mu(B_0 + B)$], respectively. The gyromagnetic ratio μ is set to 1 and g is the coupling strength. The Hamiltonian (6) applies to the ferromagnetic YIG sphere only when $g < g_c \equiv \sqrt{\omega_c \omega_m}/2$ [96]. Beyond the critical point g_c, the system remains in the superradiant phase.

The metrological scheme is shown in Fig. 1(b), where the initial magnon-cavity state is prepared in the product state $\hat{\rho}_{\rm cm}(0) = \hat{\rho}_c(0) \otimes \hat{\rho}_m(0)$. Over time, the information of the weak field B becomes encoded in the state $\hat{\rho}_{\rm cm}(t) = \exp(-iHt)\hat{\rho}_{\rm cm}(0)\exp(iHt)$. At time t_*, we perform Gaussian measurements on the cavity state $\hat{\rho}_c(t_*) = {\rm Tr}_m[\hat{\rho}_{\rm cm}(t_*)]$ and estimate the value of B from the measurement results.

Far away from critical dynamics. When $|\omega_c - \omega_m| \ll 1$ and $g \ll g_c$, we can employ the rotating-wave approximation (6) to rewrite the Hamiltonian as

$$\hat{H} = \omega_c \hat{c}^\dagger \hat{c} + \omega_m \hat{b}^\dagger \hat{b} + g(\hat{c}^\dagger \hat{b} + \hat{c}\hat{b}^\dagger). \tag{7}$$

Its dissipative dynamics is described by the quantum Langevin equations

$$\begin{aligned} \partial_t \hat{c}(t) &= -i\omega_c \hat{c}(t) - ig\hat{b}(t) - \frac{\kappa_c}{2}\hat{c}(t) + \sqrt{\kappa_c}\hat{c}_{\rm in}(t), \\ \partial_t \hat{b}(t) &= -i\omega_m \hat{b}(t) - ig\hat{c}(t) - \frac{\kappa_m}{2}\hat{b}(t) + \sqrt{\kappa_m}\hat{b}_{\rm in}(t), \end{aligned} \tag{8}$$

where κ_c and κ_m denote the damping rates of the cavity mode and the magnon mode, respectively. The input noises are described by the annihilation operators $\hat{c}_{\rm in}$ and $\hat{b}_{\rm in}$, satisfying $\langle \hat{c}_{\rm in}^\dagger(t_1)\hat{c}_{\rm in}(t_2)\rangle = n_c\delta(t_1 - t_2)$ and $\langle \hat{b}_{\rm in}^\dagger(t_1)\hat{b}_{\rm in}(t_2)\rangle = n_m\delta(t_1 - t_2)$. Here the values of n_c and n_m are subject to external environment thermal noise. For simplicity, we assume $\kappa_m = \kappa_c$ and $n_m = n_c$.

The initial state is chosen with the cavity in the vacuum state $|0\rangle$ and the magnon in a squeezed vacuum state $\hat{\rho}_m(0) = \hat{S}(r_0)|0\rangle\langle 0|\hat{S}^\dagger(r_0)$, which can be generated via parametric pumping [97–99]. The quantum Langevin equation (8) is analytically solved and the evolution of $\hat{\rho}_c(t)$ can be divided into two processes [76]:

$$\hat{\rho}_c(0) \xrightarrow[\rm P1]{\text{no noise}} \hat{\rho}_{\rm in}(t) \xrightarrow[\rm P2]{\text{noise}} \hat{\rho}_c(t), \tag{9}$$

where $\hat{\rho}_{\rm in}(t)$ denotes the cavity state in the noiseless case. During the evolution the displacement of $\hat{\rho}_c(t)$ is always zero. Focusing on the corresponding covariance matrices, we find [76] the following:

$$\begin{aligned} &\text{P1:}\ \ \gamma_{\rm in}^c(t) = \xi(t)\gamma_{\rm sq}^c + [1 - \xi(t)]\mathbb{1}_2, \\ &\text{P2:}\ \ \gamma^c(t) = \eta(t)\gamma_{\rm in}^c(t) + [1 - \eta(t)](2n_c + 1)\mathbb{1}_2, \end{aligned} \tag{10}$$

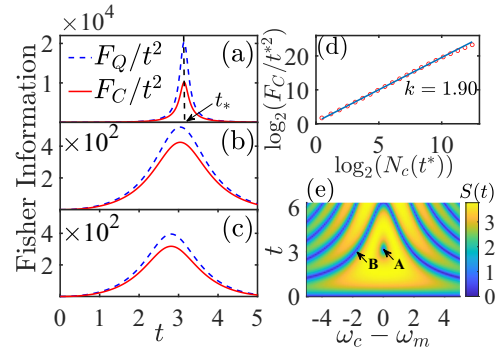

FIG. 2. Time evolution of the time-rescaled QFI F_Q/t^2 (blue dotted line) and CFI F_C/t^2 (red line) in (a) the resonance case $\omega_c = \omega_m = 2$ and $\kappa_c = n_c = 0$; (b) the dissipated case $\omega_c = \omega_m = 2$, $\kappa_c = 0.001$, and $n_c = 30$; and (c) the off-resonance case $\omega_c = 2$, $\omega_m = 2.5$, and $\kappa_c = n_c = 0$. (d) Scaling law of the CFI ($F_C \sim N_c^k$ with $k = 1.90$) for the parameter setting used in the experiment [68]: $\omega_c = \omega_m = 15.506 \times 2\pi$ GHZ, $g = 7.11 \times \pi$ GHZ, and $\kappa_c = \kappa_m = 1.029 \times \pi$ MHZ. t_* denotes the time of the CFI peak and $N_c(t_*)$ is the number of photons at that moment. (e) Time evolution of entanglement $S(t)$ versus the detuning $\omega_c - \omega_m$.

where $\gamma_{\rm sq}^c$ is the covariance matrix of the squeezed state $\hat{S}(-r_0 e^{-i(\omega_c+\omega_m)t})|0\rangle$, r_0 is the squeezing parameter of the initial magnon state, and $\gamma_{\rm in}^c(t)$ and $\gamma^c(t)$ are the covariance matrices of $\hat{\rho}_{\rm in}(t)$ and $\hat{\rho}_c(t)$, respectively. Here $\eta(t) = \exp(-\kappa_c t)$, $\xi(t) = 4g^2 \sin^2(\Delta t/2)/\Delta^2$, and $\Delta = \sqrt{4g^2 + (\omega_c - \omega_m)^2}$.

In the dissipative process P2, Eq. (10) implies that $\gamma^c(t)$ tends toward a thermal state $(2n_c + 1)\mathbb{1}_2$ since $\lim_{t\to\infty}\eta(t) = 0$. This process indicates the gradual dissipation of information into the external environment, resulting in measurement precision described by the QFI (CFI) being smaller than that in the nondissipative case [see Figs. 2(a) and 2(b)].

Unlike process P2, process P1 describes the flow of the magnetic field information between the cavity and the magnon. At $t = 0$, the cavity is only a vacuum state without any quantum resources and information. Then the appearance of the dynamics-induced bipartite entanglement essentially leads to the transmission of information from the squeezed magnon state into the cavity [see Fig. 2(e)]. From Eq. (10), we observe that the cavity state finally becomes a squeezed state $\hat{S}(-r_0 e^{-i(\omega_c+\omega_m)t})|0\rangle$ [100] at a time $t_* = \pi/(2g)$ satisfying $\xi(t_*) = 1$. This condition is satisfied only for the resonant case. It is crucial to emphasize that, at this special time t_*, the whole system $\hat{\rho}_{\rm cm}(t_*)$ is in a nonentangled state, yet both the information ω_m and the initial squeezing resource r_0 have been completely transferred to the cavity part without thermalization. Thus, the HL precision ($F_C \sim N_c^2$) can be achieved in the absence of noise by Eq. (3). Using experimental parameters [68], we show that the precision still remains near HL, specifically $F_C \sim N_c^{1.90}$ as shown in Fig. 2(d). Here, the Gilbert damping of magnons κ_m/ω_m is on the order of 10^{-3} [68,101].

If the estimated weak magnetic field $\vec{B}$ deviates from the bias field $\vec{B}_0$ along the z axis, the Hamiltonian (7) acquires an additional term, $-(B_x - iB_y)\hat{b}/2 - (B_x + iB_y)\hat{b}^\dagger/2$. In the SM [76], we show that these nonparallel

components contribute to the displacement of the evolved Gaussian state and their impact on QFI is limited to the SNL. Significantly, the nonvanishing parallel component effectively encodes information into the covariance matrix, leading to QFI following the HL. Consequently, in our subsequent discussion, we can safely disregard the nonparallel components [76]. Based on Ref. [67], crystalline anisotropy becomes notable in nanomagnets around a 2-nm radius. However, the YIG sphere considered here has a 360-nm diameter [66]. Thus, the effect of crystalline anisotropy can be disregarded.

The significance of dynamic entanglement in the encoding information process becomes clearer through a contrasting example where the inputs are magnon and cavity squeezed coherent states with identical squeezing parameters. In this setup, no bipartite entanglement will be generated, indicating that information B cannot be efficiently encoded into the phase parameter and is solely in the displacement parameter. Based on the analysis below Eq. (4), the precision cannot surpass the SNL, even in the presence of squeezing.

Returning to the initial scenario, however, entanglement during the measurement process will introduce thermalization [see Eq. (4)]. Consequently, the initial squeezing resource r_0 cannot be fully transferred to the cavity, disrupting the HL precision. Figure 2(e) shows the entanglement evolution concerning the detuning parameter $\omega_c - \omega_m$. Vanishing entanglement in the curve B (blue) indicates the quantum state periodically returns to the initial state. A nontrivial situation occurs in the resonant region A where entanglement vanishes after encoding the information into the cavity's covariance matrix, ensuring the realization of HL precision. Far away from region A, increasing detuning leads to strong entanglement between the cavity and the magnon, thus failing to suppass the SNL [see Figs. 2(a) and 2(c)].

Critical dynamics. In the strong-coupling regime, Hamiltonian (6) is directly diagonalizable as $\hat{H} = \epsilon_- \hat{c}_1^\dagger \hat{c}_1 + \epsilon_+ \hat{c}_2^\dagger \hat{c}_2$ using the Bogoliubov transformation [96]. The normal-to-superradiant phase transition occurs at the critical point $g_c = \sqrt{\omega_c \omega_m}/2$. Near this point ($g \to g_c$), the excitation energy of the photon branch scales as $\epsilon_- \sim (g_c - g)^{1/2}$ and its derivative plays a crucial role in achieving criticality-enhanced metrology. Thus, in contrast to the weak-coupling case, no specific resource state is required and we can choose the vacuum states as inputs.

Using Eqs. (1), (2), and (5), we derive the analytic expression of the covariance matrix $\gamma^c(t)$ in Ref. [76]. There is a special time $t_* = n\pi/\epsilon_-$ ($n \in \mathbb{Z}_{>0}$) at which the covariance matrix $\gamma^c(t_*)$ is finite, otherwise it diverges. It then follows from Eq. (1) that the divergence of γ^c at $t \neq t_*$ implies the divergence of the number of thermalized particles $n_{\rm th}$, e.g., $n_{\rm th}(t_*/4) \sim (g_c - g)^{-1/2}$ [76]. Therefore, by the relation (4) we find that the magnon-photon entanglement $S(t)$ becomes large at $t \neq t_*$, but almost disappears suddenly at $t = t_*$ [see Fig. 3(a)].

Figure 3(b) shows that the measurement precision has a maximum at the time t_*, meanwhile the entanglement almost disappears at $t = t_*$. In this sense, the vanishing entanglement in the measurement process enhances the measurement precision. More rigorously, we obtain critical scalings of the relevant parameters [102] and QFI:

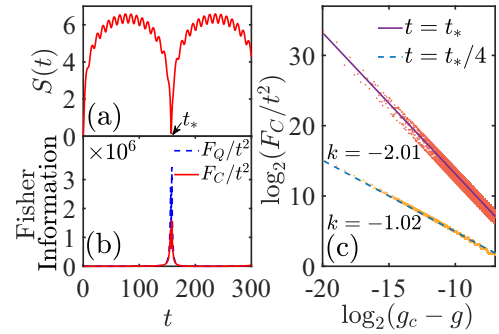

FIG. 3. Time evolution of (a) entanglement $S(t)$, (b) time-rescaled QFI F_Q/t^2, and CFI F_C/t^2 for critical dynamics. (c) Scaling of CFI: $F_C \sim (g_c - g)^k$, with $k = -2.01$ for $t = t_*$ and $k = -1.02$ for $t = t_*/4$. Lines in panel (c) are the results of fitting the theoretical data. Other parameters are $\omega_c = \omega_m = 2$, $g = 0.9999 g_c$, and $t_* = \pi/\epsilon_-$.

$$F_Q(t_*) \sim F_C(t_*) \sim (g_c - g)^{-2} t_*^2,$$
$$F_Q(t_*/4) \sim F_C(t_*/4) \sim (g_c - g)^{-1} t_*^2, \tag{11}$$

which are further confirmed by the numerical results shown in Fig. 3(c).

It is worth noting that, compared with the t_* case, the divergent squeezing [$\cosh(2r) \sim (g_c - g)^{-1/2}$] in the $t_*/4$ case causes no further enhancement in measurement precision. This is mainly because such a divergence in the covariance matrix also leads to a strong entanglement that makes the cavity state more insensitive to the estimated parameter (see the scalings of r' and ϕ' in Ref. [102]).

Conclusion. The usable bipartite entanglement in accessible metrological schemes has been established by linking Fisher information to entanglement. We have elaborated on the significance of entanglement in the efficient encoding process for high-precision quantum estimation, particularly starting from the initial product state, while unveiling the adverse impact of entanglement on the final measurement process. These findings enable us to design quantum-enhanced estimations within an experimentally feasible cavity magnonic system. In particular, we have proposed an approach to realizing the precision of the HL in the weak-coupling regime. Regarding strong coupling, we have demonstrated that the criticality-enhanced metrology should attribute to the criticality-induced parameter sensitivity rather than to criticality-induced squeezing. Our protocols show a potential application of quantum metrology through current experimental cavity magnonic systems [54,103–110], enabling quantum-enhanced metrology with or without a particular squeezed initial state.

Acknowledgments. We thank J. Yang, X.-H. Wang, and Y.-G. Su for valuable comments and suggestions. This work was supported by NSFC Key Grants No. 92365202 and No. 12134015 and by NSFC Grants No. 11874393 and No. 12121004. H.-L.S. was supported by the European Commission through the H2020 QuantERA ERA-NET Cofund in Quantum Technologies project "MENTA."

The authors Q.-K.W. and H.-L.S. contributed equally to this work.

[1] C. M. Caves, K. S. Thorne, R. W. P. Drever, V. D. Sand-berg, and M. Zimmermann, On the measurement of a weak classical force coupled to a quantum-mechanical oscillator. I. Issues of principle, Rev. Mod. Phys. **52**, 341 (1980).

[2] C. M. Caves, Quantum-mechanical noise in an interferometer, Phys. Rev. D **23**, 1693 (1981).

[3] L. Pezzé, A. Smerzi, M. K. Oberthaler, R. Schmied, and P. Treutlein, Quantum metrology with nonclassical states of atomic ensembles, Rev. Mod. Phys. **90**, 035005 (2018).

[4] V. Giovannetti, S. Lloyd, and L. Maccone, Quantum metrology, Phys. Rev. Lett. **96**, 010401 (2006).

[5] P. Hyllus, W. Laskowski, R. Krischek, C. Schwemmer, W. Wieczorek, H. Weinfurter, L. Pezzé, and A. Smerzi, Fisher information and multiparticle entanglement, Phys. Rev. A **85**, 022321 (2012).

[6] G. Tóth, Multipartite entanglement and high-precision metrology, Phys. Rev. A **85**, 022322 (2012).

[7] N. Li and S. Luo, Entanglement detection via quantum Fisher information, Phys. Rev. A **88**, 014301 (2013).

[8] Z. Ren, W. Li, A. Smerzi, and M. Gessner, Metrological detection of multipartite entanglement from young diagrams, Phys. Rev. Lett. **126**, 080502 (2021).

[9] Y. Su and X. Wang, Parametrized protocol achieving the Heisenberg limit in the optical domain via dispersive atom-light interactions, Results Phys. **24**, 104159 (2021).

[10] B. Yadin, M. Fadel, and M. Gessner, Metrological complementarity reveals the Einstein-Podolsky-Rosen paradox, Nat. Commun. **12**, 2410 (2021); Author correction: Metrological complementarity reveals the Einstein-Podolsky-Rosen paradox, *ibid.* **12**, 6481 (2021).

[11] F. Fröwis, M. Fadel, P. Treutlein, N. Gisin, and N. Brunner, Does large quantum Fisher information imply Bell correlations? Phys. Rev. A **99**, 040101(R) (2019).

[12] I. Gianani, V. Berardi, and M. Barbieri, Witnessing quantum steering by means of the Fisher information, Phys. Rev. A **105**, 022421 (2022).

[13] A. Niezgoda and J. Chwedeńczuk, Many-body nonlocality as a resource for quantum-enhanced metrology, Phys. Rev. Lett. **126**, 210506 (2021).

[14] D. Girolami, A. M. Souza, V. Giovannetti, T. Tufarelli, J. G. Filgueiras, R. S. Sarthour, D. O. Soares-Pinto, I. S. Oliveira, and G. Adesso, Quantum discord determines the interferometric power of quantum states, Phys. Rev. Lett. **112**, 210401 (2014).

[15] D. Girolami, Interpreting quantum discord in quantum metrology, J. Phys.: Conf. Ser. **626**, 012042 (2015).

[16] A. Sone, Q. Zhuang, C. Li, Y.-X. Liu, and P. Cappellaro, Nonclassical correlations for quantum metrology in thermal equilibrium, Phys. Rev. A **99**, 052318 (2019).

[17] P. Jurcevic, B. P. Lanyon, P. Hauke, C. Hempel, P. Zoller, R. Blatt, and C. F. Roos, Quasiparticle engineering and entanglement propagation in a quantum many-body system, Nature (London) **511**, 202 (2014).

[18] O. A. Castro-Alvaredo, C. De Fazio, B. Doyon, and I. M. Szécsényi, Entanglement content of quasiparticle excitations, Phys. Rev. Lett. **121**, 170602 (2018).

[19] N. Laflorencie, Quantum entanglement in condensed matter systems, Phys. Rep. **646**, 1 (2016).

[20] L. Venema, B. Verberck, I. Georgescu, G. Prando, E. Couderc, S. Milana, M. Maragkou, L. Persechini, G. Pacchioni, and L. Fleet, The quasiparticle zoo, Nat. Phys. **12**, 1085 (2016).

[21] X.-G. Wen, Colloquium: Zoo of quantum-topological phases of matter, Rev. Mod. Phys. **89**, 041004 (2017).

[22] X.-G. Wen, Choreographed entanglement dances: Topological states of quantum matter, Science **363**, eaal3099 (2019).

[23] X. Chen, Z.-C. Gu, and X.-G. Wen, Local unitary transformation, long-range quantum entanglement, wave function renormalization, and topological order, Phys. Rev. B **82**, 155138 (2010).

[24] J. Eisert, M. Friesdorf, and C. Gogolin, Quantum many-body systems out of equilibrium, Nat. Phys. **11**, 124 (2015).

[25] P. Calabrese and J. Cardy, Entanglement and correlation functions following a local quench: A conformal field theory approach, J. Stat. Mech. (2007) P10004.

[26] V. Scarani, N. Gisin, and S. Popescu, Proposal for energy-time entanglement of quasiparticles in a solid-state device, Phys. Rev. Lett. **92**, 167901 (2004).

[27] L. C. Venuti and P. Zanardi, Quantum critical scaling of the geometric tensors, Phys. Rev. Lett. **99**, 095701 (2007).

[28] P. Zanardi, M. G. A. Paris, and L. C. Venuti, Quantum criticality as a resource for quantum estimation, Phys. Rev. A **78**, 042105 (2008).

[29] S.-J. Gu, H.-M. Kwok, W.-Q. Ning, and H.-Q. Lin, Fidelity susceptibility, scaling, and universality in quantum critical phenomena, Phys. Rev. B **77**, 245109 (2008); **83**, 159905(E) (2011).

[30] A. F. Albuquerque, F. Alet, C. Sire, and S. Capponi, Quantum critical scaling of fidelity susceptibility, Phys. Rev. B **81**, 064418 (2010).

[31] S.-J. Gu, Fidelity approach to quantum phase transitions, Int. J. Mod. Phys. B **24**, 4371 (2010).

[32] I. Frérot and T. Roscilde, Quantum critical metrology, Phys. Rev. Lett. **121**, 020402 (2018).

[33] L. Garbe, M. Bina, A. Keller, M. G. A. Paris, and S. Felicetti, Critical quantum metrology with a finite-component quantum phase transition, Phys. Rev. Lett. **124**, 120504 (2020).

[34] V. Montenegro, U. Mishra, and A. Bayat, Global sensing and its impact for quantum many-body probes with criticality, Phys. Rev. Lett. **126**, 200501 (2021).

[35] Y. Chu, S. Zhang, B. Yu, and J. Cai, Dynamic framework for criticality-enhanced quantum sensing, Phys. Rev. Lett. **126**, 010502 (2021).

[36] R. Liu, Y. Chen, M. Jiang, X. Yang, Z. Wu, Y. Li, H. Yuan, X. Peng, and J. Du, Experimental critical quantum metrology with the Heisenberg scaling, npj Quantum Inf. **7**, 170 (2021).

[37] T. Ilias, D. Yang, S. F. Huelga, and M. B. Plenio, Criticality-enhanced quantum sensing via continuous measurement, PRX Quantum **3**, 010354 (2022).

[38] D. Yang, S. F. Huelga, and M. B. Plenio, Efficient Information retrieval for sensing via continuous measurement, Phys. Rev. X **13**, 031012 (2023).

[39] R. Di Candia, F. Minganti, K. V. Petrovnin, G. S. Paraoanu, and S. Felicetti, Critical parametric quantum sensing, npj Quantum Inf. **9**, 23 (2023).

[40] P. Krammer, H. Kampermann, D. Bruß, R. A. Bertlmann, L. C. Kwek, and C. Macchiavello, Multipartite entanglement detection via structure factors, Phys. Rev. Lett. **103**, 100502 (2009).

[41] P. Hauke, M. Heyl, L. Tagliacozzo, and P. Zoller, Measuring multipartite entanglement through dynamic susceptibilities, Nat. Phys. **12**, 778 (2016).

[42] A. V. Chumak, V. I. Vasyuchka, A. A. Serga, and B. Hillebrands, Magnon spintronics, Nat. Phys. **11**, 453 (2015).

[43] B. Lenk, H. Ulrichs, F. Garbs, and M. Münzenberg, The building blocks of magnonics, Phys. Rep. **507**, 107 (2011).

[44] H. Y. Yuan, Y. Cao, A. Kamra, R. A. Duine, and P. Yan, Quantum magnonics: When magnon spintronics meets quantum information science, Phys. Rep. **965**, 1 (2022).

[45] B. Z. Rameshti, S. V. Kusminskiy, J. A. Haigh, K. Usami, D. Lachance-Quirion, Y. Nakamura, C.-M. Hu, H. X. Tang, G. E. W. Bauer, and Y. M. Blanter, Cavity magnonics, Phys. Rep. **979**, 1 (2022).

[46] Y. Li, W. Zhang, V. Tyberkevych, W.-K. Kwok, A. Hoffmann, and V. Novosad, Hybrid magnonics: Physics, circuits, and applications for coherent information processing, J. Appl. Phys. **128**, 130902 (2020).

[47] M. Harder, B. M. Yao, Y. S. Gui, and C.-M. Hu, Coherent and dissipative cavity magnonics, J. Appl. Phys. **129**, 201101 (2021).

[48] J. Li, S.-Y. Zhu, and G. S. Agarwal, Magnon-photon-phonon entanglement in cavity magnomechanics, Phys. Rev. Lett. **121**, 203601 (2018).

[49] X. Zhang, C.-L. Zou, L. Jiang, H. X. Tang, Cavity magnomechanics, Sci. Adv. **2**, e1501286 (2016).

[50] M. Yu, H. Shen, and J. Li, Magnetostrictively induced stationary entanglement between two microwave fields, Phys. Rev. Lett. **124**, 213604 (2020).

[51] H. Y. Yuan, P. Yan, S. Zheng, Q. Y. He, K. Xia, and M.-H. Yung, Steady Bell state generation via magnon-photon coupling, Phys. Rev. Lett. **124**, 053602 (2020).

[52] H. Huebl, C. W. Zollitsch, J. Lotze, F. Hocke, M. Greifenstein, A. Marx, R. Gross, and S. T. B. Goennenwein, High cooperativity in coupled microwave resonator ferrimagnetic insulator hybrids, Phys. Rev. Lett. **111**, 127003 (2013).

[53] D. Lachance-Quirion, S. P. Wolski, Y. Tabuchi, S. Kono, K. Usami, and Y. Nakamura, Entanglement-based single-shot detection of a single magnon with a superconducting qubit, Science **367**, 425 (2020).

[54] S. P. Wolski, D. Lachance-Quirion, Y. Tabuchi, S. Kono, A. Noguchi, K. Usami, and Y. Nakamura, Dissipation-based quantum sensing of magnons with a superconducting qubit, Phys. Rev. Lett. **125**, 117701 (2020).

[55] Ö. O. Soykal and M. E. Flatté, Strong field interactions between a nanomagnet and a photonic cavity, Phys. Rev. Lett. **104**, 077202 (2010).

[56] M. Elyasi, Y. M. Blanter, and G. E. W. Bauer, Resources of nonlinear cavity magnonics for quantum information, Phys. Rev. B **101**, 054402 (2020).

[57] Z. Zhang, M. O. Scully, and G. S. Agarwal, Quantum entanglement between two magnon modes via Kerr nonlinearity driven far from equilibrium, Phys. Rev. Res. **1**, 023021 (2019).

[58] V. A. Mousolou, Y. Liu, A. Bergman, A. Delin, O. Eriksson, M. Pereiro, D. Thonig, and E. Sjöqvist, Magnon-magnon entanglement and its quantification via a microwave cavity, Phys. Rev. B **104**, 224302 (2021).

[59] H. Y. Yuan, S. Zheng, Z. Ficek, Q. Y. He, and M.-H. Yung, Enhancement of magnon-magnon entanglement inside a cavity, Phys. Rev. B **101**, 014419 (2020).

[60] G. M. Andolina, M. Keck, A. Mari, M. Campisi, V. Giovannetti, and M. Polini, Extractable work, the role of correlations, and asymptotic freedom in quantum batteries, Phys. Rev. Lett. **122**, 047702 (2019).

[61] J.-X. Liu, H.-L. Shi, Y.-H. Shi, X.-H. Wang, and W.-L. Yang, Entanglement and work extraction in the central-spin quantum battery, Phys. Rev. B **104**, 245418 (2021).

[62] H.-L. Shi, S. Ding, Q.-K. Wan, X.-H. Wang, and W.-L. Yang, Entanglement, coherence, and extractable work in quantum batteries, Phys. Rev. Lett. **129**, 130602 (2022).

[63] V. Montenegro, M. G. Genoni, A. Bayat, and M. G. A. Paris, Probing of nonlinear hybrid optomechanical systems via partial accessibility, Phys. Rev. Res. **4**, 033036 (2022).

[64] V. Montenegro, M. G. Genoni, A. Bayat, and M. G. A. Paris, Mechanical oscillator thermometry in the nonlinear optomechanical regime, Phys. Rev. Res. **2**, 043338 (2020).

[65] Y. Tabuchi, S. Ishino, T. Ishikawa, R. Yamazaki, K. Usami, and Y. Nakamura, Hybridizing ferromagnetic magnons and microwave photons in the quantum limit, Phys. Rev. Lett. **113**, 083603 (2014).

[66] X. Zhang, C.-L. Zou, L. Jiang, and H. X. Tang, Strongly coupled magnons and cavity microwave photons, Phys. Rev. Lett. **113**, 156401 (2014).

[67] Ö. O. Soykal, and M. E. Flatté, Size dependence of strong coupling between nanomagnets and photonic cavities, Phys. Rev. B **82**, 104413 (2010).

[68] J. Bourhill, N. Kostylev, M. Goryachev, D. L. Creedon, and M. E. Tobar, Ultrahigh cooperativity interactions between magnons and resonant photons in a YIG sphere, Phys. Rev. B **93**, 144420 (2016).

[69] Here, $\hat{D}(\alpha) = \exp(\alpha\hat{c}^\dagger - \bar{\alpha}\hat{c})$ is the displacement operator, $\hat{S}(\zeta) = \exp(-\zeta\hat{c}^{\dagger 2}/2 + \bar{\zeta}\hat{c}^2/2)$ is the squeezing operator with $\zeta = r\exp(i\phi)$, and $\hat{\rho}_{\rm th} = \sum_n P_n|n\rangle\langle n|$ is a thermal state with $P_n = n_{\rm th}^n/(1+n_{\rm th})^{1+n}$ and $|n\rangle$ is the Fock state.

[70] G. Adam, Density matrix elements and moments for generalized Gaussian state fields, J. Mod. Opt. **42**, 1311 (1995).

[71] C. R. Rao, Information and the accuracy attainable in the estimation of statistical parameters, Bull. Calcutta Math. Soc. **37**, 81 (1945).

[72] H. Cramér, *Mathematical Methods of Statistics* (Princeton University, Princeton, NJ, 1946).

[73] C. W. Helstrom, Minimum mean-squared error of estimates in quantum statistics, Phys. Lett. A **25**, 101 (1967).

[74] J. Liu, H. Yuan, X.-M. Lu, and X. Wang, Quantum Fisher information matrix and multiparameter estimation, J. Phys. A: Math. Theor. **53**, 023001 (2020).

[75] The expression of the quantum Fisher information for general Gaussian states has been obtain in terms of the covariance matrix and the displacement vector: O. Pinel, P. Jian, N. Treps, C. Fabre, and D. Braun, Quantum parameter estimation using general single-mode Gaussian states, Phys. Rev. A **88**,

040102(R) (2013); A. Monras, Phase space formalism for quantum estimation of Gaussian states, arXiv:1303.3682.

[76] See Supplemental Material at http://link.aps.org/supplemental/10.1103/PhysRevB.109.L041301 for details of the calculation of Eqs. (2), (5), (10), and (11).

[77] M. G. A. Paris, Quantum estimation for quantum technology, Int. J. Quantum Inf. **07**, 125 (2009).

[78] B. C. Hall, Lie groups, Lie algebras, and representations: An elementary introduction, Graduate Texts in Mathematics (Springer, Berlin, 2015), Vol. 222.

[79] V. V. Dodonov, 'Nonclassical' states in quantum optics: A 'squeezed' review of the first 75 years, J. Opt. B: Quantum Semiclassical Opt. **4**, R1 (2002).

[80] J. N. Hollenhorst, Quantum limits on resonant-mass gravitational-radiation detectors, Phys. Rev. D **19**, 1669 (1979).

[81] D. F. Walls, Squeezed states of light, Nature (London) **306**, 141 (1983).

[82] K. McKenzie, D. A. Shaddock, D. E. McClelland, B. C. Buchler, and P. K. Lam, Experimental demonstration of a squeezing-enhanced power-recycled Michelson interferometer for gravitational wave detection, Phys. Rev. Lett. **88**, 231102 (2002).

[83] K. McKenzie, N. Grosse, W. P. Bowen, S. E. Whitcomb, M. B. Gray, D. E. McClelland, and P. K. Lam, Squeezing in the audio gravitational-wave detection band, Phys. Rev. Lett. **93**, 161105 (2004).

[84] H. Vahlbruch, S. Chelkowski, B. Hage, A. Franzen, K. Danzmann, and R. Schnabel, Demonstration of a squeezed-light-enhanced power- and signal-recycled Michelson interferometer, Phys. Rev. Lett. **95**, 211102 (2005).

[85] H. Vahlbruch, S. Chelkowski, B. Hage, A. Franzen, K. Danzmann, and R. Schnabel, Coherent control of vacuum squeezing in the gravitational-wave detection band, Phys. Rev. Lett. **97**, 011101 (2006).

[86] The number of photons is given by $N_c = \langle \hat{c}^\dagger \hat{c} \rangle = |\alpha|^2 + n_{\rm th} + (2n_{\rm th}+1)\sinh^2 r$. The quantum squeezing-induced contribution to the number of photons is $\sinh^2 r \sim \exp(2r)$. If we further consider the impact of thermalization, we can assume $n_{\rm th} \sim e^{\nu r}$, analogous to the quantum squeezing-induced contribution. The exact solution of the quantum dynamics governed by the Hamiltonian (7) also confirmed this assumption, see the Supplemental Material [76].

[87] V. Vedral, M. B. Plenio, M. A. Rippin, and P. L. Knight, Quantifying entanglement, Phys. Rev. Lett. **78**, 2275 (1997).

[88] G. S. Agarwal, Entropy, the Wigner distribution function, and the approach to equilibrium of a system of coupled harmonic oscillators, Phys. Rev. A **3**, 828 (1971).

[89] A. Monras, Optimal phase measurements with pure Gaussian states, Phys. Rev. A **73**, 033821 (2006).

[90] R. J. Rossi, *Mathematical Statistics: An Introduction to Likelihood Based Inference* (Wiley & Sons, New York, 2018).

[91] C. Weedbrook, S. Pirandola, R. García-Patrón, N. J. Cerf, T. C. Ralph, J. H. Shapiro, and S. Lloyd, Gaussian quantum information, Rev. Mod. Phys. **84**, 621 (2012).

[92] G. Giedke and J. I. Cirac, Characterization of Gaussian operations and distillation of Gaussian states, Phys. Rev. A **66**, 032316 (2002).

[93] J. Eisert and M. B. Plenio, Introduction to the basics of entanglement theory in continuous-variable systems, Int. J. Quantum Inf. **01**, 479 (2003).

[94] T. Holstein and H. Primakoff, Field dependence of the intrinsic domain magnetization of a ferromagnet, Phys. Rev. **58**, 1098 (1940).

[95] This Hamiltonian is similar to the one considered in S. Kotler, A. Peterson, E. Shojaee, F. Lecocq, K. Cicak, A. Kwiatkowski, S. Geller, S. Glancy, E. Knill, R. W. Simmonds, J. Aumentado, and J. D. Teufel, Direct observation of deterministic macroscopic entanglement, Science **372**, 622 (2021); L. Mercier de Lépinay, C. F. Ockeloen-Korppi, M. J. Woolley, and M. A. Sillanpää, Quantum mechanics-free subsystem with mechanical oscillators, *ibid.* **372**, 625 (2021).

[96] C. Emary and T. Brandes, Chaos and the quantum phase transition in the Dicke model, Phys. Rev. E **67**, 066203 (2003).

[97] J. Li, S.-Y. Zhu, and G. S. Agarwal, Squeezed states of magnons and phonons in cavity magnomechanics, Phys. Rev. A **99**, 021801(R) (2019).

[98] S. O. Demokritov, V. E. Demidov, O. Dzyapko, G. A. Melkov, A. A. Serga, B. Hillebrands, and A. N. Slavin, Bose-Einstein condensation of quasi-equilibrium magnons at room temperature under pumping, Nature (London) **443**, 430 (2006).

[99] W. Zhang, D.-Y. Wang, C.-H. Bai, T. Wang, S. Zhang, and H.-F. Wang, Generation and transfer of squeezed states in a cavity magnomechanical system by two-tone microwave fields, Opt. Express **29**, 11773 (2021).

[100] Note that $\gamma_{\rm sq}^c$ is the covariance matrix of the squeezed state $\hat{S}(-r_0 e^{-i(\omega_c+\omega_m)t})|0\rangle$ in Eq. (10).

[101] G. Wu, Y. Cheng, S. Guo, F. Yang, D. V. Pelekhov, and P. C. Hammel, Nanoscale imaging of Gilbert damping using signal amplitude mapping, Appl. Phys. Lett. **118**, 042403 (2021).

[102] Here the scalings of the thermalization and squeezing parameters are explicitly given by $n_{\rm th} \sim (g_c - g)^0$, $\cosh(2r) \sim (g_c - g)^0$, $n'_{\rm th} \sim (g_c - g)^{-1} t_*$, $\phi' \sim (g_c - g)^{-1} t_*$, and $r' \sim (g_c - g)^{-1} t_*$ for $t = t_*$ and by $n_{\rm th} \sim (g_c - g)^{-1/2}$, $\cosh(2r) \sim (g_c - g)^{-1/2}$, $n'_{\rm th} \sim (g_c - g)^{-1} t_*$, $\phi' \sim (g_c - g)^0 t_*$, and $r' \sim (g_c - g)^{-1/2} t_*$ for $t = t_*/4 = \pi/(4\epsilon_-)$. Details can be found in the Supplemental Material [76]. Entanglement is positively related to $n_{\rm th}$.

[103] M. Silaev, Ultrastrong magnon-photon coupling and entanglement in superconductor/ferromagnet nanostructures, Phys. Rev. B **107**, L180503 (2023).

[104] J. W. Rao, B. Yao, C. Y. Wang, C. Zhang, T. Yu, and W. Lu, Unveiling a pump-induced magnon mode via its strong interaction with Walker modes, Phys. Rev. Lett. **130**, 046705 (2023).

[105] I. A. Golovchanskiy, N. N. Abramov, V. S. Stolyarov, A. A. Golubov, M. Yu. Kupriyanov, V. V. Ryazanov, and A. V. Ustinov, Approaching deep-strong on-chip photon-to-magnon coupling, Phys. Rev. Appl. **16**, 034029 (2021).

[106] A. F. Kockum, A. Miranowicz, S. De Liberato, S. Savasta, and F. Nori, Ultrastrong coupling between light and matter, Nat. Rev. Phys. **1**, 19 (2019).

[107] I. Boventer, M. Pfirrmann, J. Krause, Y. Schön, M. Kläui, and M. Weides, Complex temperature dependence of

coupling and dissipation of cavity magnon polaritons from millikelvin to room temperature, Phys. Rev. B **97**, 184420 (2018).

[108] I. A. Golovchanskiy, N. N. Abramov, V. S. Stolyarov *et al.*, Ultrastrong photon-to-magnon coupling in multilayered heterostructures involving superconducting coherence via ferromagnetic layers, Sci. Adv. **7**, eabe8638 (2021).

[109] N. Kostylev, M. Goryachev, M. E. Tobar, Superstrong coupling of a microwave cavity to yttrium iron garnet magnons, Appl. Phys. Lett. **108**, 062402 (2016).

[110] D. Xu, X.-K. Gu, H.-K. Li, Y.-C. Weng, Y.-P. Wang, J. Li, H. Wang, S.-Y. Zhu, and J. Q. You, Quantum control of a single magnon in a macroscopic spin system, Phys. Rev. Lett. **130**, 193603 (2023).